

MM Science Journal | www.mmscience.eu

ISSN 1803-1269 (Print) | ISSN 1805-0476 (On-line)

Special Issue | HSM 2025 18th International Conference on High Speed Machining

October 15-16, 2025, Metz, France DOI: 10.17973/MMSJ.2025_11_2025138



HSM2025-44843

ANALYSIS OF THE FRICTION AND WEAR MECHANISMS AT THE TOOL-WORKPIECE CONTACT UNDER EXTREME CONTACTS LOADINGS AND HIGH SLIDING SPEEDS

N.Haterbouch^{1*}, H.Makich¹, A.Cappella¹, H.Ben Boubaker¹, M.Nouari¹ ¹Universite de Lorraine, CNRS, Arts et Metiers Institute of Technology, LEM3, F-57000 Metz, France *N.Haterbouch; Email: najwa.haterbouch@univ-lorraine.fr

Abstract

Friction and wear significantly degrade cutting tools and surface quality of machined parts in high-speed machining. This study examines the Ti-6Al-4V/WC-Co contacts under a range of PV (pressure × velocity) of (160-4000 MPa.m/s) with contacting pressures of 64,110,200 and 320 MPa and sliding speeds of 0.5,1,10 and 20 m/s. These contact conditions are representative of the tool-workpiece and tool-chip contacts when machining titanium alloys by cemented carbide tools. The low-speed tests were carried out on conventional test bench using a pin-on-disc configuration, while high-speed tests were made on a gas-gun device. Friction coefficients, wear measurements, and high-resolution surface analyses were performed for each condition to analyze the contact between tool and workpiece under a large range of sliding speed and pressure. The results reveal a transition from an adhesive-dominated wear mechanism at high pressures and low speeds to tribo-oxidative and abrasive mechanisms at elevated sliding speeds. In a large range of contact conditions, a non-linear dependence of the friction law on contact pressure and sliding velocity parameters was found.

Keywords:

Contact, Extreme loading, Friction, Wear characterization

1 INTRODUCTION

Titanium alloy Ti-6Al-4V (TA6V) is extensively used in aerospace, biomedical, and high-performance engineering sectors due to its good properties (high strength-to-weight ratio, excellent corrosion resistance, and superior However, biocompatibility) [Philip 2019]. advantageous properties are not conducive to a good machinability of materials. Moreover, this titanium alloy exhibits low thermal conductivity, high chemical reactivity with cutting tools, and a strong tendency to work-hardening, leading then to a rapid tool wear and high cutting forces, during machining process [Patil 2015], [Bammidi 2023].

Cemented carbide-cobalt (WC-Co) composites are among the most commonly used materials for cutting tools when machining the Ti-6Al-4V alloy due to their exceptional hardness, toughness, and heat resistance [Agode 2022]. Despite this, WC-Co tools suffer from severe adhesive and diffusive wear mechanisms when machining titanium alloys, especially for industrial applications where contact pressures often reach 1-3 GPa and sliding speeds range from 10 to 60 m/min (0.1-1 m/s) [Ezugwu 1997].

Understanding the tribological interaction between Ti-6Al-4V and WC-Co materials at the tool-chip and toolworkpiece interfaces is therefore essential for improving machining performance and tool life longevity. In literature, tribological studies have shown that the contact between the tool and chip during machining is not uniform and can be divided into several distinct zones. Ackroyd et al. [Ackroyd 2003] reported four zones: a stagnation zone, a retardation zone, a sliding zone, and a sticking zone. These zones are characterized by varying sliding velocities and contact pressures, with highest velocities typically observed toward the end of contact. Moreover, the nature of friction and heat partitioning at the tool-chip interface is strongly dependent on the local sliding velocity. As sliding speed increases, the contact transitions between different frictional regimes, affecting both pressure distribution and thermal behavior. In contrast, the tool-workpiece interface is typically characterized by a high initial contact pressure that gradually decreases as the cutting process evolves and the chip begins to form.

While some studies have employed tribometer setups to investigate the frictional response of TA6V, relatively few have focused explicitly on the Ti-6Al-4V/WC-Co interface. For instance, Niu et al. [Niu 2013] studied WC-Co/Ti-6Al-4V contacts under dry conditions and found that adhesion and abrasive wear dominate at low pressures and speeds.

Other studies extended this analysis to high sliding speed conditions for the same alloy. Philippon et al. [Philippon 2004] observed that friction increased with speed up to 13 m/s before decreasing due to thermal softening and oxide film formation. Ming et al. [Ming 2006] identified a critical velocity of 40 m/s beyond which adhesive wear and friction

MM SCIENCE JOURNAL I 2025 I Special Issue on HSM2025

rise sharply. Chassaing et al. [Chassaing 2014] demonstrated that even at moderate contact pressures (110 MPa), high-speed impact results in progressive adhesive wear and sub-surface structural transformations.

Furthermore, test configuration and contact geometry significantly affect tribological response. While point or line contacts concentrate stress and interrupt sliding, flat-on-flat setups provide more uniform pressure distributions and uninterrupted motion, better simulating machining interfaces. Baydoun et al. [Baydoun 2019] introduced a frictional energy model for flat-on-flat steel contacts, correlating film breakdown and wear to a threshold in accumulated frictional energy. Liang et al. [Liang 2020] further applied flat-on-flat testing to Ti-6Al-4V/WC-Co pairs and noted a friction coefficient drop from 0.56 to 0.3 as temperature increased, due to surface softening of the titanium.

The current study investigates friction and wear mechanisms of Ti-6Al-4V/WC-10Co couple under contact conditions with pressure P ranging from 64 to 320 MPa and sliding speed V ranging from 0.5 to 20 m/s). These conditions are representative of the two contact zones between tool and workpiece, and between tool and chip. Using complementary flat-on-flat tribometer setups: a quasi-static pin-on-disc and a pad-on-slider tribometer. This work explores how contact pressure and sliding velocity govern wear regimes and microstructural transformations.

The paper is structured as follows: Section 2 describes the materials and experimental setup; Section 3 presents results and discussions; Section 4 outlines the main conclusions and future directions.

2 EXPERIMENTAL PROCEDRURE

2.1 Experimental setup

The study investigates the tribological behavior of Ti6Al4V against WC-10%Co under three distinct frictional regimes designed to replicate interface conditions between tool and machined materials:

- (1) an adhesive-dominated regime (Condition A) simulating high-pressure (320 MPa), low-speed (0.5 1 m/s) interactions at the tool-workpiece interface,
- (2) a sliding/abrasive-dominated regime (Condition B) representing low-pressure (110-200 MPa), high-speed (20 m/s) conditions at the tool-chip interface,
- (3) a transitional regime (Condition C) at intermediate speed (10 m/s) and pressure (64 MPa).

These conditions were examined through two specialized tribological configurations: a pin-on-disc tribometer as shown in Fig.1 for conditions A and C, and a high-speed slider-on-pads tribometer using a gas-gun device as shown in Fig.2 for condition B.

The experimental matrix shown in Tab. 1 was designed to isolate the effects of the sliding speed (V) and the contact pressure (P) while maintaining representative PV (pressure \times velocity) conditions. For the adhesive regime, tests at fixed high pressure (320 MPa) evaluated speed effects (V = 0.5 m/s and 1 m/s). The abrasive regime employed fixed high speed (20 m/s) to assess pressure variations (P = 110 MPa and 200 MPa). The transitional condition (V = 10 m/s, P = 64 MPa) provided intermediate data points, ensuring comprehensive coverage of the tribological response across operational parameters. Each test configuration was repeated twice to ensure reproducibility.

Tab.1. Sliding test conditions.

Condition	Contact pressure	Sliding speed	PV
	(MPa)	(m/s)	(MPa.m/s)
Α	320	0.5	160
	320	1	320
В	110	20	2200
	200	20	4000
С	64	10	640

Pin-on-disc configuration

The first configuration shown in Fig.1 is a pin-on-disc tribometer BRUKER® UMT TriboLab, was used for low to moderate speeds. It features bi-axial force sensors (Z: 1-2000 N, X: 1-1000 N, 0.1 N accuracy) and a high-torque motor (0.1-5000 rpm). Tests began once the pin contacted the rotating disc under a steady normal load. The system continuously recorded friction forces and calculated the coefficient of friction.

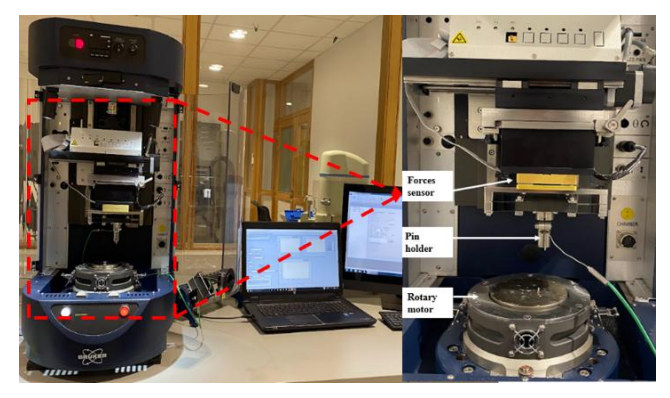


Fig. 1. Pin on disc tribometer configuration.

Slider-on-pads configuration (gas-gun device)

As shown in Fig.2 a second configuration, a slider-on-pads impact tribometer, was used for high-speed tests. A projectile impacted a slider fixed between pads, generating brief sliding motion. Force sensors captured normal and tangential forces, and high-speed instrumentation recorded frictional data.



Fig. 2. Slider-on-pads tribometer configuration.

2.2 Experimental procedure

Both configurations employed a flat-on-flat contact geometry to maintain quasi-static pressure distribution. However, the contact area differs between the two setups. In low-speed tests, a 6 mm diameter hemispherical WC-Co pin (2 mm tip radius) contacted a 70 mm diameter Ti-6Al-4V disc, resulting in a nominal contact area of 3.14 mm². For high-speed tests, a Ti-6Al-4V slider (50 × 8 × 3 mm) slides against WC-Co pads (20 × 12 × 5 mm), producing an apparent contact area of 30 mm².

The samples were prepared by polishing Ti6Al4V discs with abrasive paper to minimize surface roughness effects. The

WC-Co pins and pads (10% cobalt) were selected for their wear resistance.

A post-processing script calculated the average coefficient of friction (COF) during the steady-state regime, using filtered normal and tangential force data.

Surface characterization was conducted using a scanning electron microscope (SEM, ZEISS Supra 40) equipped with Secondary Electron (SE2) and Backscattered Electron (BSD) detectors, allowing for the examination of wear features and microstructural alterations. Elemental analysis of transferred materials was performed qualitatively using an Energy-Dispersive X-ray Spectroscopy (EDS) system. Prior to SEM analysis, the samples were ultrasonically cleaned in an acetone-ethanol solution.

3 RESULTS AND DISCUSSIONS

3.1 Friction behavior across tribological regimes

The tribological behavior of the Ti6Al4V/WC-Co system was systematically investigated under the five test conditions discussed in Tab.1, which were classified into three representative regimes based on the pressure-velocity (PV) product: an adhesive-dominated regime (Condition A, PV = 160-320 MPa·m/s), a sliding/abrasive-dominated regime (Condition B, PV = 2200-4000 MPa·m/s), and a transitional regime (Condition C, PV = 640 MPa·m/s). Conditions A and C were investigated using the pin-on-disc tribometer (Fig. 1), whereas Condition B was examined with the slider-on-pads configuration (Fig. 2).

As illustrated in Fig. 3, the coefficient of friction (COF) demonstrated a non-monotonic dependence on PV, reflecting a complex interplay of mechanical and thermal effects.

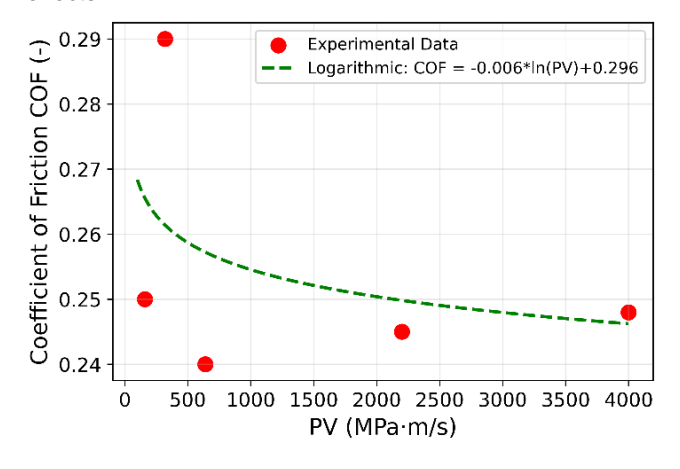


Fig.3. Coefficient of Friction (COF) as a function of PV (MPa·m/s): Experimental study and logarithmic modeling.

The maximum COF (0.293) occurred under low PV conditions, characteristic of strong adhesive interactions induced by high contact pressure (320 MPa) and low sliding speeds (0.5-1 m/s). These conditions promote stable asperity junctions and localized plastic deformation, in line with classical contact theories [Archard, 1953] and consistent with prior studies reporting similar COF values in the range of 0.24-0.3 under comparable parameters. Niu et al. studied a ball on flat WC-Co/Ti-6Al-4V test under a sliding speed of 0.112 m/s, they found that the friction coefficient initially increased from 0.24 to 0.32 before stabilizing at 0.42 over time with fluctuations [Niu 2013]. Interestingly, more severe adhesion and higher COF values (up to 0.56) have been observed by Liang et al. [Liang 2020]

in flat-on-flat pin-on-disc configurations at very low speeds than 0.5m/s, at 0.1 m/s they highlighted the sensitivity of interfacial behavior to contact geometry. In contrast, Condition B (PV = 2200-4000 MPa·m/s) exhibited a reduced COF of 0.245 ± 0.005, indicative of a transition toward a sliding and abrasive-dominated regime. Here, high sliding speeds (20 m/s) likely facilitated the formation of tribo-oxidative layers through frictional heating, thereby lowering interfacial shear strength. This behavior aligns with findings by Philippon et al. [Philippon 2004] who reported friction reduction at velocities above 13 m/s due to the increase in temperature in the contact zone leading to the emergence of oxide films acting as solid lubricants. Notably, although contact pressure increased within this regime (110-200 MPa), the friction coefficient exhibited a low rise of 17%, suggesting that thermally activated mechanisms may override pressure-induced adhesion effects at elevated speeds.

The intermediate condition (Condition C), characterized by a sliding speed of 10 m/s and low pressure of 64 MPa, yielded a COF of 0.236 ± 0.017 , reflecting a mixed regime in which micro-ploughing, partial junction formation, and incipient oxide development likely coexisted. These observations underscore the inadequacy of evaluating frictional behavior based only on pressure or velocity in isolation; rather, the PV product, and by extension, cumulative frictional energy, emerges as a more reliable predictor of tribological transitions, as suggested by Baydoun et al. [Baydoun 2019].

Overall, the results reveal a progressive shift from adhesive dominated to sliding/oxidative regimes with increasing PV, governed by a nuanced balance of mechanical interlocking, thermal dissipation, and surface chemistry. A detailed analysis of wear mechanisms and surface morphology through SEM and EDX will be presented in the following section to further clarify these transitions.

3.2 Microstructural evolution and wear mechanisms

To better understand the wear mechanisms governing the Ti-6Al-4V/WC-Co tribo-system, scanning electron microscopy (SEM) and energy dispersive X-ray Spectroscopy (EDS) analyses were conducted under three representative conditions corresponding to distinct frictional regimes. The microstructural evolution observed across these regimes reveals a progressive transition from mechanically dominated wear to thermally activated degradation.

Under condition A (320 MPa, 0.5m/s and 1 m/s), the Ti-6Al-4V disc surface in fig.4(a) and fig.5(a) exhibited deep ploughing grooves aligned with the sliding direction, alongside plastic flow and evidence of abrasive wear. The WC-Co pin surface for each test of condition A, showed a thick, inhomogeneous tribo-layer formed by transferred titanium alloy, with flaking zones, edge cracking, directional abrasion marks (Fig.5(b)) and decohesion of WC-Co particles at the edges especially at the lowest speed of 0.5m/s (Fig.4(b)). These are characteristics indicative of severe plastic deformation and strong adhesive interactions. These features reflect repeated asperity junction formation and shear-induced material transfer, consistent with classical adhesive-abrasive mechanisms discussed in section 3.1.

In contrast, for condition C (64 MPa, 10 m/s), the disc surface shown in fig.6(a) was covered by a tribo-layer exhibiting multidirectional cracking and fragmented debris which is indicative of significant thermal softening.

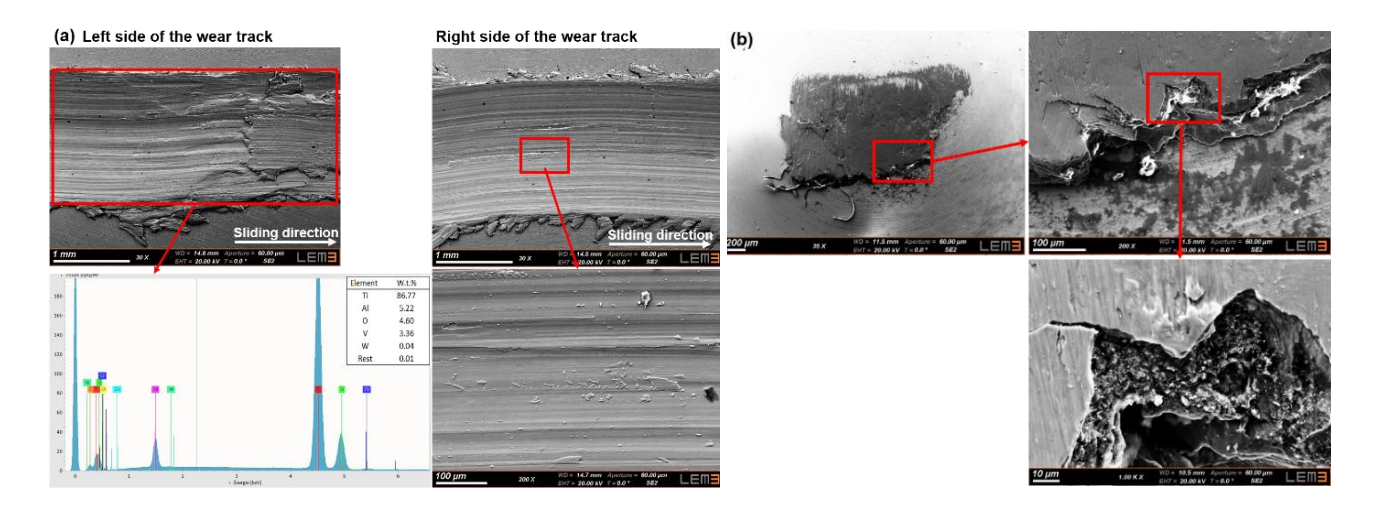


Fig.4. SEM images of the wear track under P = 320 MPa, V = 0.5 m/s, (a) Ti-6AI-4V disc, (b) WC-10Co pin.

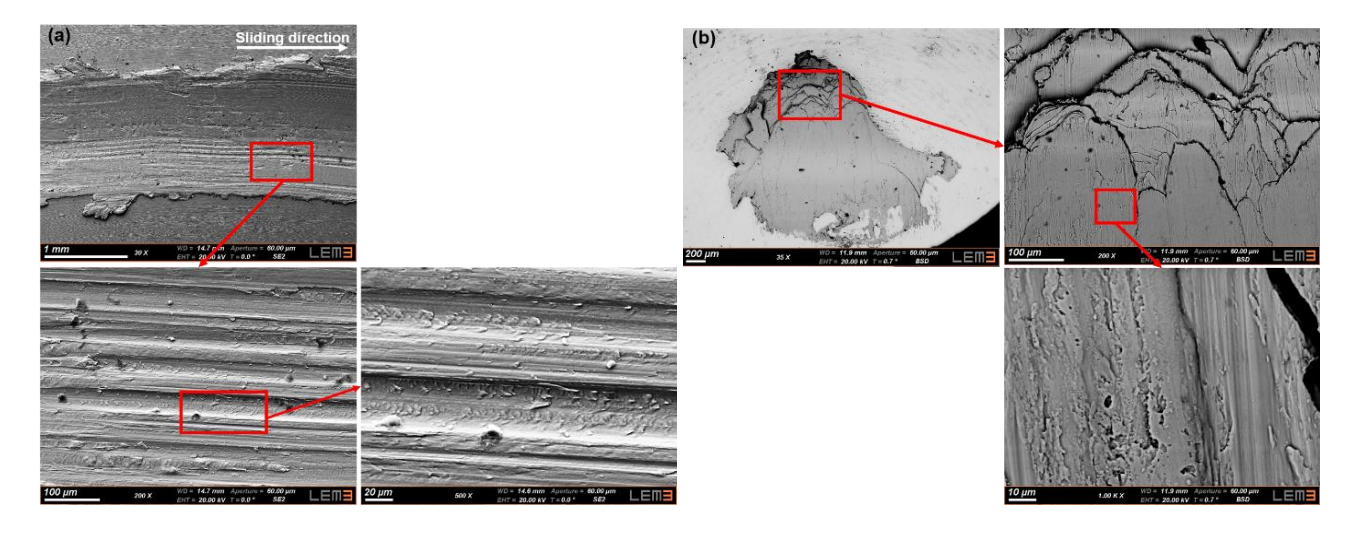


Fig.5. SEM images of the wear track under P = 320 MPa, V = 1 m/s, (a) Ti-6Al-4V disc, (b) WC-10Co pin.

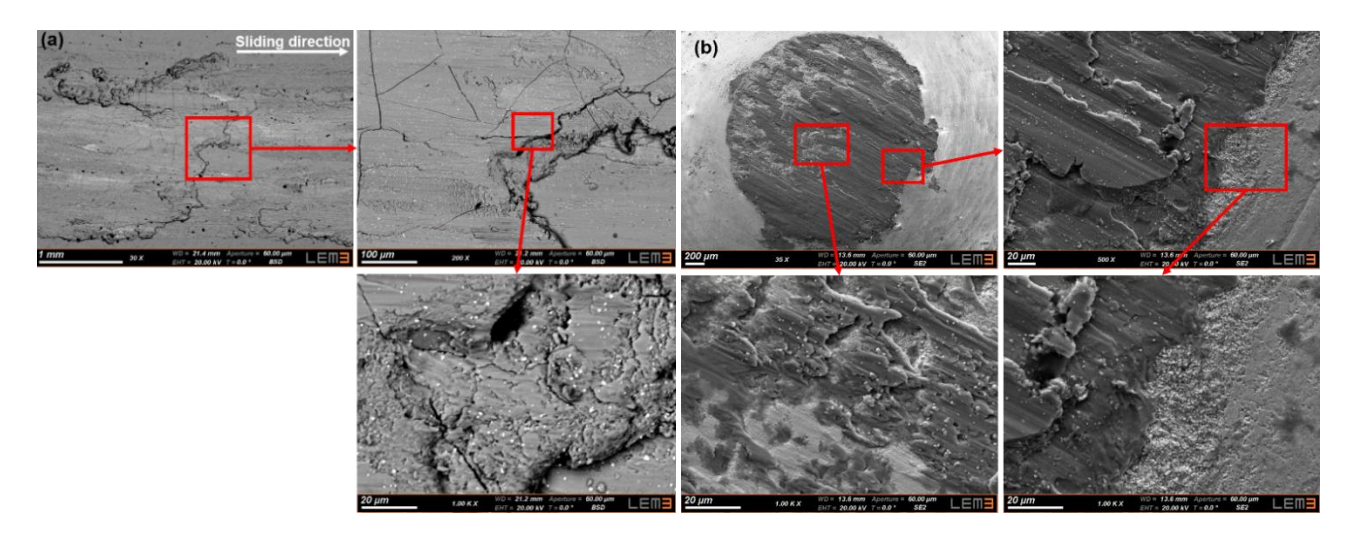


Fig.6. SEM images of the wear track under P = 64 MPa, V = 10 m/s, (a) Ti-6Al-4V disc, (b) WC-10Co pin.

Simultaneously, EDS analysis of the pin surface in fig.7 which revealed the presence of embedded tungsten carbide particles up to 43 wt.% W, suggesting that elevated sliding speed induced frictional heating sufficient to weaken or partially melt the cobalt binder in the WC-Co matrix as seen at the edge of the pin (Fig.6(b)). This thermal

degradation promoted the decohesion and liberation of WC grains, which were then either transferred into the titanium surface or entrapped during sliding, an observation that marks a transitional regime driven by thermally assisted wear processes.

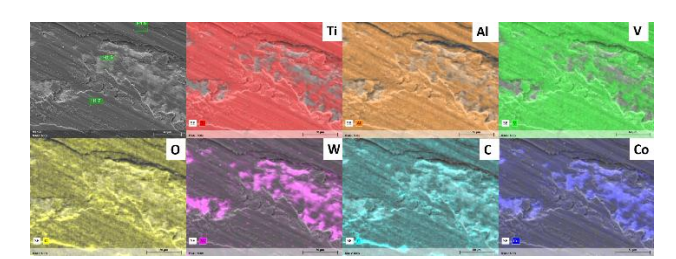


Fig.7. EDS analysis of the wear track on the WC-Co pin (zoomed area), at P = 64 MPa and V = 10 m/s.

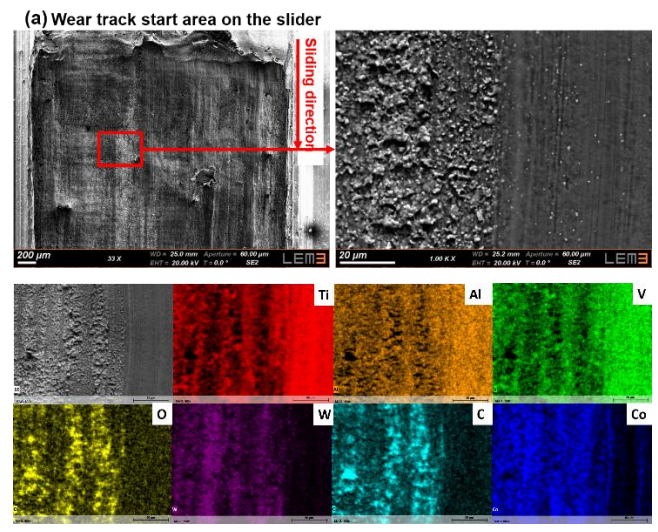
Finally, under Condition B (200 MPa, 20 m/s), the combined effects of high contact pressure and elevated sliding speed significantly transform the wear behavior of both the pad and slider surfaces. SEM observations of the pad (Fig. 8 (b)) reveal a titanium alloy transfer layer characterized by non-oriented, stress-relaxation cracks which are features commonly associated with rapid thermal cycling and planar stress dissipation, as noted by Bahr et al. [Bahr 1986]. Meanwhile, the wear track area on the slider shown in Fig.8(a) exhibits pronounced wear marked by WC-Co adhesion, its matrix decohesion, and carbide particle pull-out. At the start of the wear track, EDS analysis (Fig. 8(a)) confirms the presence of oxidized debris, indicating that high-speed friction promotes the transient formation and eventual breakdown of oxide films.

These findings collectively point to a shift in wear mechanism: from adhesion-abrasion dominance to a thermally driven regime where oxidation, cobalt binder degradation, and severe abrasive interactions become predominant. High contact pressure and velocity synergistically degrade surface stability. Overall, the evolution of microstructural features across the PV spectrum underscores a transition from adhesive-abrasive to oxidative-abrasive wear, governed by increasing thermal inputs that destabilize the WC-Co matrix and modify interfacial dynamics.

4 SUMMARY

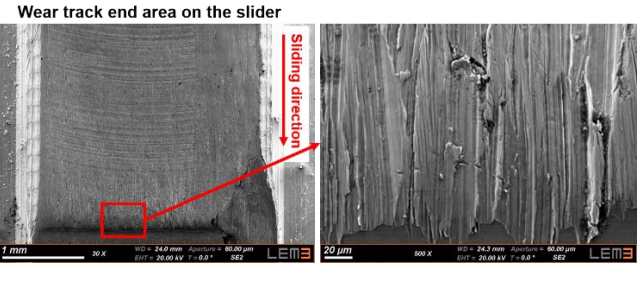
This paper studies the friction and wear behavior of the Ti-6Al-4V titanium alloy against WC-Co under a wide range of contact pressures and sliding speeds, simulating extreme tribological conditions encountered in high-speed machining process. Two complementary experimental configurations, a quasi-static pin-on-disc tribometer and a slider-on-pads tribometer configuration were employed to cover the PV values from 160 to 4000 MPa·m/s. It can be concluded that:

- Three distinct wear regimes were identified: adhesive at low PV values, transitional at moderate PV and tribo-oxidative at high PV. Each regime was characterized by unique surface damage features and friction responses.
- Friction coefficient behavior was non-linear, decreasing as function of PV factor due to the transition from plastic deformation and adhesion to oxidative film formation and micro-abrasion.
- Wear mechanisms evolved from severe plastic flow and material transfer at low speeds to brittle oxide fragmentation and debris-induced abrasion at high speeds.



Wear track middle area on the slider

| Siding Girection | City |



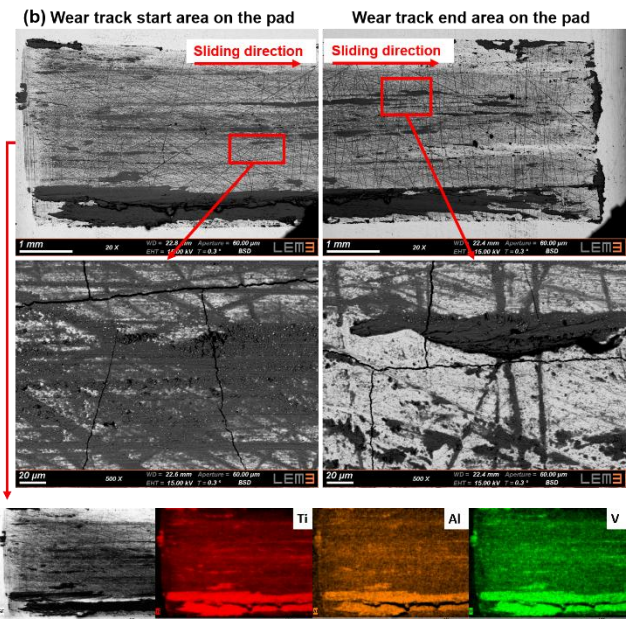


Fig.8. SEM images of the wear track under P = 200 MPa, V = 20 m/s, (a) three areas of Ti-6Al-4V slider (start, middle, end); (b) WC-10Co pad.

Future investigations will aim to quantitatively evaluate wear rates under the regimes studied here in order to refine the relationships between frictional behavior and underlying microstructural changes. The experimental design will be broadened to test a wider range of sliding velocities, alongside the integration of key parameters such as temperature and ambient environment.

5 REFERENCES

[Philip 2019] Philip, J.T. Tribology of Ti6Al4V: A review. Friction, 2019, 7(6), 497-536.

[Patil 2015] Patil, A. and S. N. Amit. Machining challenges in Ti-6Al-4V - a review. International Journal of Innovations in Engineering and Technology (IJIET), 2015, 5(4), 6-23.

[Bammidi 2023] Bammidi, R.S. Towards an understanding of Ti-6Al-4V machining and machinability. Materials Today: Proceedings, 2023.

[Agode 2022] Agode, K.E. Analysis and modeling of the wear behavior of tungsten carbide cutting tools for different cobalt contents during the machining of the titanium alloy Ti-6Al-4V. 2022.

[Ezugwu 1997] Ezugwu, E.O. and Wang, Z.M. Titanium alloys and their machinability -a review. Journal of Materials Processing Technology, 1997, 68(3), 262-274.

[Ackroyd 2003] Ackroyd, B., Chandrasekar, S. and Compton, W.D. A model for the contact conditions at the chip-tool interface in machining. Journal of Tribology, 2003, 125(3), 649-660.

[Niu 2013] Niu, Q.L. and Cui, X.H. Friction and wear performance of titanium alloys against tungsten carbide under dry sliding and water lubrication. Tribology Transactions, 2013, 56(1), 101-108.

[Philippon 2004] Philippon, S., Sutter, G. and Molinari, A. An experimental study of friction at high sliding velocities. Wear, July 2004, 257(7-8), 777-784.

[Ming 2006] Ming, Q., Yang, Z., Huang, H. and Zhang, J. Microstructure and tribological characteristics of Ti-6Al-4V alloy against GCr15 under high speed and dry sliding. Materials Science and Engineering: A, 2006, 434(1-2), 71-75

[Chassaing 2014] Chassaing, G. and Forestier, L. Adhesive wear of a Ti6Al4V tribopair for a fast friction contact. Wear, 2014, 320(1-2), 25-33.

[Baydoun 2019] Baydoun, S.F. and Fouvry, S. Fretting wear rate evolution of a flat-on-flat low alloyed steel contact: A weighted friction energy formulation. Wear, 2019, 426-427, 676-693.

[Liang 2020] Liang, X.L. Physic-chemical analysis for high-temperature tribology of WC-6Co against Ti-6Al-4V by pinon-disc method. Tribology International, 2020, 146, 106242.

[Archard 1953] Archard, J.F. Contact and rubbing of flat surfaces. Journal of Applied Physics, 1953, 24(8), 981-988.

[Bahr 1986] Bahr, H.-A. and Gerlach, J.F. Thermal-shock crack patterns explained by single and multiple crack propagation. Journal of Materials Science, 1986, 21, 2716-2720.